

Majorana dc Josephson current mediated by a quantum dot

Luting Xu,¹ Xin-Qi Li,^{1,*} and Qing-Feng Sun^{2,3,†}

¹Center for Advanced Quantum Studies and Department of Physics,
Beijing Normal University, Beijing 100875, China

²International Center for Quantum Materials, School of Physics, Peking University, Beijing 100871, China

³Collaborative Innovation Center of Quantum Matter, Beijing 100871, China

The Josephson supercurrent through the hybrid Majorana–quantum dot–Majorana junction is investigated. We particularly analyze the effect of spin-selective coupling between the Majorana and quantum dot states, which emerges only in the topological phase and will influence the current through bent junctions and/or in the presence of magnetic fields in the quantum dot. We find that the characteristic behaviors of the supercurrent through this system are quite counterintuitive, remarkably differing from the resonant tunneling, e.g., through the similar (normal phase) superconductor–quantum dot–superconductor junction. Our analysis is carried out under the influence of full set-up parameters and for both the 2π and 4π periodic currents. The present study is expected to be relevant to future exploration of applications of the Majorana-nanowire circuits.

PACS numbers:

I. INTRODUCTION

Majorana fermions (MFs) are exotic self-Hermitian particles with non-Abelian statistics, hold a property with themselves as their own antiparticles^{1–3} and promise robust building blocks for topological quantum computation^{4,5}. Remarkable insight predicts that MFs can emerge as novel excitations of Majorana zero modes or Majorana bound states in condensed matter systems, e.g., from the non-Abelian excitations in a $5/2$ fractional quantum Hall effect in semiconductor heterostructures⁶, and based on exotic superconductors where MFs correspond to zero-energy states of an effective Bogoliubov-de Gennes Hamiltonian^{7,8}.

More recent proposals employ the proximity effect from a conventional superconductor, either in nanowires in the presence of strong spin-orbit interaction and Zeeman splitting^{9–15}, or in topological insulators^{16–20}. These efforts bring the MFs closer to experimental realization and predict more reliable experimental signatures of their presence. Among the signatures include such as the half-integer conductance quantization²¹, the zero-bias peak in the tunneling conductance^{22–25}, and the 4π Josephson effect in superconductor-superconductor junctions^{14,26–28}. In particular, in order to distinguish MFs from other quasi-particle states, some interest in recent years turns to the *spin selective* Andreev reflection^{29–32}.

In this work we consider the hybrid system of Majorana–quantum dot–Majorana junction which can be realized from semiconductor nanowires in proximity-contact with *s*-wave superconductors, as schematically shown in Fig. 1. Similar systems of Majorana nanowire coupled to quantum dots (QDs) have been investigated for phenomena such as teleportation³³, anomaly of conductance peak³⁴, characteristic signatures in current noise spectrum³⁵, and featured Josephson current¹⁵. Our present interest is the dc Josephson current under the influence of spin-selective coupling between the Majorana and QD states, which is most relevant to *bent junctions*

and the presence of magnetic field in the QD area.

Due to the helical property of MF, the MF at the end of the nanowire only couples to a unique spin state in the normal region, e.g., the spin-up QD state as shown in Fig. 1. Actually, this spin-selective coupling is the origin of the spin-dependent Andreev reflection^{29,36}. In previous studies, the set-up configuration is usually assumed to be either a single Majorana nanowire coupled to normal leads or QDs, or a straight Majorana–normal region–Majorana junction with bent angle $\theta = 0$. In both cases, only the spin-up states (in the normal parts) couple to the MF and contribute to the current. However, if the Majorana–QD–Majorana junction is not straight (with a bent angle $\theta \neq 0$ between the nanowires), the two MFs at the ends of the nanowires (see Fig. 1) will couple to spin states in the QD with different orientations, leading thus to both the spin-up and spin-down states participating in the transport. This is anticipated to result in different current behaviors of the straight and bent junctions. On the application aspect (e.g. in the topological quantum computations), the Majorana nanowires will possibly have an orientational angle, or one would like to employ this orientational angle to modulate the charge transfer properties. This makes thus the bending structure studied in this work relevant to possible real circuits.

We will also analyze the effect of magnetic fields in the QD area. This is motivated by viewing that, in order to induce the emergence of MF, magnetic fields are needed to apply in the nanowires, which must spill over in the QD area owing to its close separations from the nanowires. Similar to the consequence of junction bending, we expect that the non-*z*-axial direction magnetic field will make the spin-down state involved in the transport as well. We will show that, remarkably, owing to the spin-selective coupling, both the magnetic field in the QD area and the junction bending will result in some counterintuitive behaviors of the Josephson current. For instance, in the case of QD level aligned with the Fermi en-

ergy (under resonant tunneling), the Josephson current is to be strongly suppressed by the magnetic field and junction bending. However, as the QD level deviates from the Fermi level (violates the resonant-tunneling condition), the oscillation amplitude of the Josephson current always shows an enhanced value, together with robust jumps in the current-phase curves.

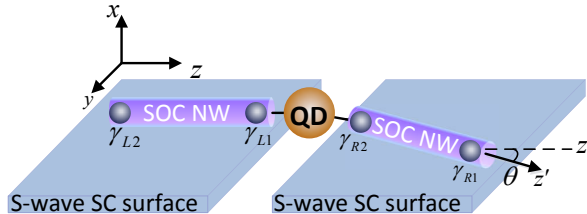


FIG. 1: (color online) Set-up sketch of the Majorana-QD-Majorana junction, realized by semiconductor nanowires in contact with the *s*-wave superconductors. The two nanowires may have a mutual orientation angle which is expected to affect the supercurrent via the unique spin-selective coupling between the Majorana and QD states.

II. MODEL AND METHODS

A. Set-up Model

In this work we consider the simple setup as shown in Fig. 1, where two semiconductor nanowires are connected through a QD. The nanowires are in proximity contacted with an *s*-wave superconductor. Then, the proximity-effect-caused superconductivity, together with the strong Rashba spin-orbit coupling (SOC) and Zeeman splitting inside the nanowires, can possibly induce emergence of a pair of MFs at the ends of each nanowire^{13,14}, as denoted in Fig. 1 by $\gamma_{L1,2}$ for the left wire and $\gamma_{R1,2}$ for the right one.

The tunnel-coupled system can be modeled by an effective low-energy Hamiltonian $H = H_M + H_{dot} + H_{dL} + H_{dR}$, more explicitly with

$$H_M = i\varepsilon_L\gamma_{L1}\gamma_{L2} + i\varepsilon_R\gamma_{R1}\gamma_{R2}, \quad (1a)$$

$$H_{dot} = \sum_{\sigma} \varepsilon_d d_{\sigma}^{\dagger} d_{\sigma} + (d_{\uparrow}^{\dagger}, d_{\downarrow}^{\dagger}) \vec{\sigma} \cdot \vec{B} \begin{pmatrix} d_{\uparrow} \\ d_{\downarrow} \end{pmatrix}, \quad (1b)$$

$$H_{dL} = (\lambda_L d_{\uparrow} - \lambda_L^* d_{\downarrow}^{\dagger}) \gamma_{L1}, \quad (1c)$$

$$H_{dR} = i(\lambda_R \tilde{d}_{\uparrow} + \lambda_R^* \tilde{d}_{\downarrow}^{\dagger}) \gamma_{R2}. \quad (1d)$$

Here H_M is the effective low energy Hamiltonian for the two pairs of Majorana states emerged at the ends of the two nanowires. Each Majorana pair may have nonzero coupling energy, i.e., $\varepsilon_L \sim e^{-l_L/\xi_L}$ and $\varepsilon_R \sim e^{-l_R/\xi_R}$, where $l_{L(R)}$ and $\xi_{L(R)}$ are, respectively, the length of the nanowire and the superconductor coherence length. H_{dot} denotes the QD Hamiltonian, with a single spatially quantized level ε_d (tunable by gate voltage), and

possibly affected via the Zeeman effect by magnetic field $\mathbf{B} = (B_x, B_y, B_z)$ (Here we assume an arbitrary direction of magnetic field). d_{σ}^{\dagger} and d_{σ} are the creation and annihilation operators of the QD electron with spin σ .

H_{dL} and H_{dR} describe the tunnel coupling between the dot and the nearby Majorana states. In general, the coupling amplitudes can be expressed as $\lambda_{L(R)} = |\lambda_{L(R)}| e^{i\phi_{L(R)}/2}$, where the phase factors are determined by the phase of the substrate superconductors and their difference will result in the famous Josephson current. Another important issue to be noted is that, due to the helical property of MF, the MF only couples to the spin-up state in the QD (defined in the same *z*-representation of the associated nanowire)^{29,36}. As mentioned in the introduction, our special interest in this work is to consider the two nanowires not aligned in the same orientation, but with an angle θ , as shown in Fig.1. Thus, the left and right MFs would couple only to the QD state spin-polarized, respectively, along the *z* and *z'* axes, with the associated electron operators connected by the following unitary transformation:

$$\begin{pmatrix} \tilde{d}_{\uparrow} \\ \tilde{d}_{\downarrow} \end{pmatrix} = \begin{pmatrix} \cos \frac{\theta}{2} & \sin \frac{\theta}{2} \\ -\sin \frac{\theta}{2} & \cos \frac{\theta}{2} \end{pmatrix} \begin{pmatrix} d_{\uparrow} \\ d_{\downarrow} \end{pmatrix}. \quad (2)$$

This implies that, if the bent angle $\theta \neq 0$, the spin-down state also couples to the MFs.

In practice, it would be convenient to convert the MFs to regular fermion representation, via the simple transformation: $c_L = (\gamma_{L1} + i\gamma_{L2})/\sqrt{2}$, and $c_R = (\gamma_{R1} + i\gamma_{R2})/\sqrt{2}$. The creation operators are their Hermitian conjugate and satisfy $\{c_{L(R)}, c_{L(R)}^{\dagger}\} = 1$. Now let us apply the generalized Nambu representation, by introducing the field creation and annihilation operators as $\psi^{\dagger} = (d_{\uparrow}^{\dagger}, d_{\downarrow}^{\dagger}, d_{\downarrow}, d_{\uparrow}, c_L^{\dagger}, c_L, c_R^{\dagger}, c_R)$, and $\psi = (d_{\uparrow}, d_{\downarrow}, d_{\downarrow}^{\dagger}, d_{\uparrow}^{\dagger}, c_L, c_L^{\dagger}, c_R, c_R^{\dagger})^T$. Then, the Hamiltonian of the whole system can be rewritten as

$$H = \frac{1}{2} \psi^{\dagger} \mathcal{H} \psi, \quad (3)$$

where the Hamiltonian matrix has a block form given by

$$\mathcal{H} = \begin{pmatrix} \mathcal{H}_{dd} & \mathcal{H}_{dL} & \mathcal{H}_{dR} \\ \mathcal{H}_{Ld} & \mathcal{H}_{LL} & 0 \\ \mathcal{H}_{Rd} & 0 & \mathcal{H}_{RR} \end{pmatrix}, \quad (4)$$

and each sub-matrix reads, respectively,

$$\mathcal{H}_{dd} = \begin{pmatrix} \varepsilon_d + B_z & B_x - iB_y & 0 & 0 \\ B_x + iB_y & \varepsilon_d - B_z & 0 & 0 \\ 0 & 0 & -\varepsilon_d + B_z & -B_x + iB_y \\ 0 & 0 & -B_x - iB_y & -\varepsilon_d - B_z \end{pmatrix}, \quad (5a)$$

$$\mathcal{H}_{LL} = \begin{pmatrix} \varepsilon_L & 0 \\ 0 & -\varepsilon_L \end{pmatrix}, \quad (5b)$$

$$\mathcal{H}_{RR} = \begin{pmatrix} \varepsilon_R & 0 \\ 0 & -\varepsilon_R \end{pmatrix}, \quad (5c)$$

$$\mathcal{H}_{dL} = \frac{1}{\sqrt{2}} \begin{pmatrix} -\lambda_L^* & -\lambda_L^* \\ 0 & 0 \\ 0 & 0 \\ \lambda_L & \lambda_L \end{pmatrix}, \quad (5d)$$

$$\mathcal{H}_{dR} = \frac{1}{\sqrt{2}} \begin{pmatrix} \lambda_R^* \cos \frac{\theta}{2} & -\lambda_R^* \cos \frac{\theta}{2} \\ \lambda_R^* \sin \frac{\theta}{2} & -\lambda_R^* \sin \frac{\theta}{2} \\ \lambda_R \sin \frac{\theta}{2} & -\lambda_R \sin \frac{\theta}{2} \\ \lambda_R \cos \frac{\theta}{2} & -\lambda_R \cos \frac{\theta}{2} \end{pmatrix}. \quad (5e)$$

The other two off-diagonal sub-matrices are given by $\mathcal{H}_{Ld} = \mathcal{H}_{dL}^\dagger$ and $\mathcal{H}_{Rd} = \mathcal{H}_{dR}^\dagger$.

B. Josephson current

From the description of the above low-energy effective Hamiltonian, it seems that this system, which accommodates discrete energy levels, can support only unitary evolution (quantum oscillations). However, this is not true. Note that the MFs at the ends of the nanowire are induced via contact with superconductor which has the Cooper pair reservoir. Even under zero bias voltage, the both superconductors (see Fig. 1) can support stationary dc Josephson current, if a phase difference between the superconductors is maintained. This understanding allows us to apply the quantum transport formalism of nonequilibrium Green's function (nGF) to the present set-up with only discrete energy levels.

Following the nGF technique outlined in Ref. [37,38], the Josephson current reads

$$I = \frac{e}{h} \int d\epsilon \text{Re Tr} \{ \tilde{\sigma}_z [\tilde{\Sigma}(\epsilon) G_d(\epsilon)]^< \}. \quad (6)$$

This result is expressed in the Nambu representation. Accordingly, $\tilde{\sigma}_z = \text{diag}\{1, 1, -1, -1\}$, which makes the Keldysh equation $[\tilde{\Sigma} G_d]^< = \tilde{\Sigma}^< G_d^a + \tilde{\Sigma}^r G_d^<$ applicable in the compact form. G_d is the ‘reduced’ effective Green's function of the quantum dot, by accounting for the effect of the ‘leads’ (the Majoranas connected at both sides) as self-energies (as usual in the nGF formalism for transport). Here we use $\tilde{\Sigma}$ to denote the difference of the self-energies from the left and right wires (leads), $\tilde{\Sigma} = \Sigma_L - \Sigma_R$. The associated retarded and advanced self-energies are given, respectively, by

$$\Sigma_{L/R}^{r(a)}(\epsilon) = \mathcal{H}_{dL/R} g_{L/R}^{r(a)}(\epsilon) \mathcal{H}_{L/Rd} \quad (7)$$

where $g_{L/R}^{r(a)}(\epsilon) = [\epsilon - \mathcal{H}_{LL/RR} \pm i0^+]^{-1}$ are the retarded (advanced) Green's functions of the isolated left/right wires. For the lesser self-energies, one can apply: $\Sigma_{L/R}^<(\epsilon) = f(\epsilon)[\Sigma_{L/R}^a(\epsilon) - \Sigma_{L/R}^r(\epsilon)]$, where $f(\epsilon)$ is the Fermi-Dirac distribution function. The retarded and advanced Green's functions read $G_d^{r(a)}(\epsilon) = [\epsilon - \mathcal{H}_{dd} - (\Sigma_L^r + \Sigma_R^a)]^{-1}$, and the lesser Green's function can be similarly obtained by using $G_d^<(\epsilon) = f(\epsilon)[G_d^a(\epsilon) - G_d^r(\epsilon)]$. Using these relations together with some algebras, we obtain

$$I = \frac{e}{h} \int d\epsilon \text{Re Tr} [\tilde{\sigma}_z (\tilde{\Sigma}^a G_d^a - \tilde{\Sigma}^r G_d^r)] f(\epsilon). \quad (8)$$

This compact formula will be applied in this work to calculate the Josephson current.

III. RESULTS

In the numerical investigations, results will be calculated under the influence of a couple of set-up parameters: the gate voltage, which would affect the QD level ε_d ; the bent angle θ of the junction; the magnetic field in the QD area; and the overlap strength of the Majorana wavefunctions ($\varepsilon_{L/R}$). We would like to set $|\lambda_L| = |\lambda_R| = \lambda = 1$ and scale all energies by λ . Also, we denote the Fermi level of the entire set-up as reference (zero) energy, the phase difference between the superconductors as $\Delta\phi = \phi_R - \phi_L$, and assume zero temperature and identical nanowires ($\varepsilon_L = \varepsilon_R$).

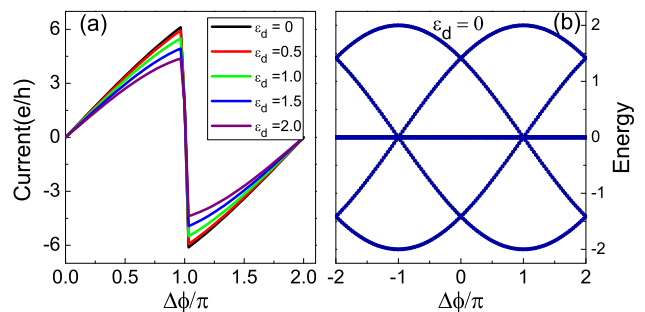


FIG. 2: (color online) (a) Josephson current *versus* the phase difference between the two superconductors for the straight Majorana–QD–Majorana junction ($\theta = 0$), under modulation of the QD energy level. The parameters $\varepsilon_L = \varepsilon_R = 0$ and the magnetic field $\mathbf{B} = 0$. (b) Example of the associated in-gap energy diagram of the Josephson junction in the topological phase, which can help us understand the current behavior shown in (a).

A. Effect of Dot Level Modulation

We first display the result for the straight junction with $\theta = 0$. In this case, the unique Majorana feature is revealed, as shown in Fig. 2(a), by the robust ‘jump’ of

the Josephson current at $\Delta\phi = \pi$ and the non-vanishing current when modulating the dot level ε_d (via modulation of the gate voltage applied). We see that, with the increase of ε_d (even far away from the Fermi energy, i.e., $\varepsilon_d = 0$), the Josephson current only reduces by a small amount, and the jump at $\Delta\phi = \pi$ always survives there, being robust against the variation of ε_d . For instance, for $\varepsilon_d = 2.0$, the amplitude of the Josephson current is only reduced to about 70% of the value at $\varepsilon_d = 0$.

The both features revealed here are entirely different from the normal superconductor-QD-superconductor junction. In the normal (trivial) case, the jump only appears at $\varepsilon_d = 0$ and the current is to be strongly suppressed when ε_d deviates far away from the Fermi energy³⁸. We thus conclude that the features revealed in Fig. 2(a) are closely associated with the superconductor-proximity-induced nontrivial (topological) phase of the nanowire where the MF emerges. In this case, the structure of the energy diagram is as shown in Fig. 2(b), where we find the remarkable zero-energy crossing points at $\Delta\phi = \pm\pi$ which are responsible for the current “jumps” as observed in Fig. 2(a).

Qualitatively speaking, the current is the sum of all contributions from the occupied energy levels, with each individual proportional to the derivative of the associated energy curve (with respect to $\Delta\phi$)²⁶. In this work, we calculate the current using Eq. (8). We integrate the energy from $-\infty$ to the Fermi level, implying that the system is always in thermal equilibrium especially when $\Delta\phi$ passes through π . This treatment corresponds to certain relaxation mechanism involved, as a consequence of *particle addition/loss* from/to the surrounding environment. As a consequence, we obtain the 2π periodic current (as a function of $\Delta\phi$), Fig. 2(a). Only under the fermion-number-parity conservation, the so-called 4π periodic current can be expected. We will address this issue later in more detail.

B. Effect of Magnetic Fields

We now consider the possible effects of magnetic field in the dot area. For the Zeeman splitting of the dot level caused by the magnetic field along the z axis, we can understand that the effect is the same as the electric gate-modulation of the dot level, as shown in Fig. 2(a).

The effect of B_x (magnetic field along the x axis) is shown in Fig. 3. For the ideal configuration with $\varepsilon_d = 0$, the jump at $\Delta\phi = \pi$ disappears and evolves to a rounded transition behavior. And, with the increase of B_x , the Josephson current quickly decreases and vanishes at last.

For $\varepsilon_d \neq 0$, similar modulation effect of B_x on the amplitude of the Josephson current is caused by the spin-selective coupling between the Majorana and QD states, by noting that the magnetic field B_x has a role of rotating the electron spin, leading thus to a change of the z -

component of the spin. However, in this more “relaxed” case ($\varepsilon_d \neq 0$), the jump behavior at $\Delta\phi = \pi$ survives. This indicates that the Majorana characteristic *jump* behavior is robust against the deviation of the dot level from the Fermi energy, even under the influence of magnetic field in the QD area.

Moreover, out of simple expectation, if the dot level ε_d is far away from the Fermi energy (e.g. $\varepsilon_d = 1$), the Josephson current is reduced by B_x much more modestly, than in the case of $\varepsilon_d = 0$, see, e.g., the results in Fig. 3(a) and (d). Indeed, this behavior is very counterintuitive, since in usual case the largest current always appears at resonant tunneling^{39,40}, i.e., the dot level ε_d at the Fermi energy.

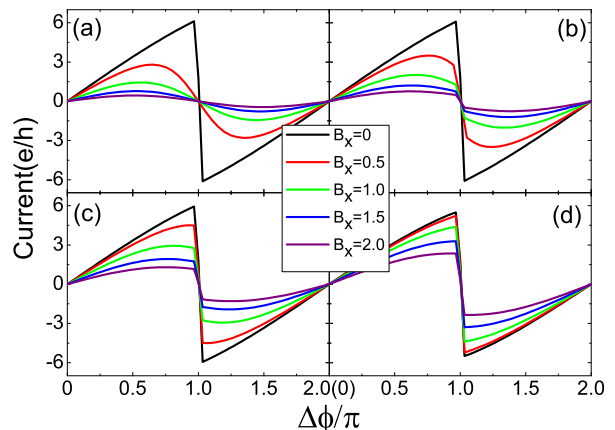


FIG. 3: (color online) Current-phase behavior under the influence of the x -component of the magnetic field in the dot area. Results for several locations of the dot level are displayed: (a) $\varepsilon_d = 0$; (b) $\varepsilon_d = 0.2$; (c) $\varepsilon_d = 0.5$; and (d) $\varepsilon_d = 1.0$.

C. Effect of Junction Bending

As remarked in the Introduction, the spin-selective coupling can be manifested also by bending the junction, i.e., by altering the mutual angle (θ) between the nanowires. The results are displayed in Fig. 4, which actually resemble what we observed in Fig. 3. That is, the “jump” at $\Delta\phi = \pi$ is rounded in Fig. 4(a) for $\varepsilon_d = 0$, while in Fig. 4(b), (c), and (d) for $\varepsilon_d \neq 0$, the “jump” survives and the maximum (amplitude) of the current decreases with the increase of the bent angle θ . Again, out of expectation, for finite θ (e.g. $\theta = \frac{\pi}{4}$, $\frac{\pi}{2}$ and $\frac{3\pi}{4}$), the amplitude of the Josephson current would increase with the deviation of the dot level from the Fermi energy. This means that, for a bent Majorana-Josephson junction, the stronger the resonance condition is violated, a larger supercurrent will flow through the junction. We finally mention that, for all cases, the parameter $\theta = \pi$ simply means rotating the right wire to the same side of

the quantum dot and in parallel to the left wire, which would result in a completely vanished current.

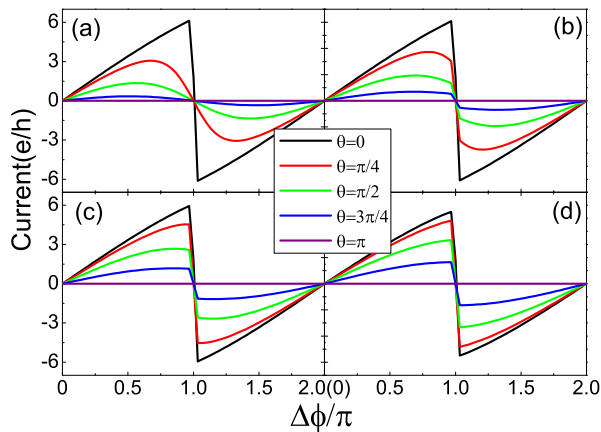


FIG. 4: (color online) Effect of junction bending on the current-phase behavior. Displayed are results for several locations of the dot level: (a) $\varepsilon_d = 0$; (b) $\varepsilon_d = 0.2$; (c) $\varepsilon_d = 0.5$; and (d) $\varepsilon_d = 1.0$.

D. Energy Diagram Based Interpretation

We found through Figs. 2, 3 and 4 that, regardless of the magnetic field \mathbf{B} and the mutual angle θ , the current jump can safely survive and the amplitude of the current maintains a large value, if the dot level ε_d violates the resonance condition. We may further understand the behaviors as follows, with the help of the energy diagrams of Fig. 2(b) and Fig. 5.

First, in Fig. 2(b) for $\varepsilon_d = 0$ and $\theta = 0$, the flat zero-energy level are of four-fold degeneracy, i.e., for the states

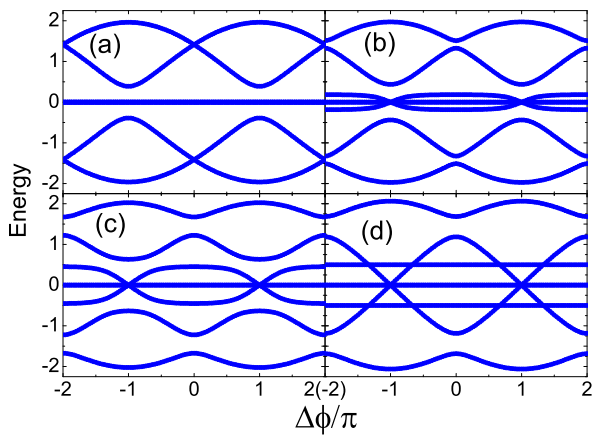


FIG. 5: (color online) Energy diagram of the junction for a couple of set-up parameters: (a) $\varepsilon_d = 0$, $\theta = 0.25\pi$; (b) $\varepsilon_d = 0.2$, $\theta = 0.25\pi$; (c) $\varepsilon_d = 0.5$, $\theta = 0.25\pi$; and (d) $\varepsilon_d = 0.5$, $\theta = 0$.

γ_{L2} , γ_{R1} , d_{\downarrow} and d_{\downarrow}^{\dagger} . The other four phase-difference ($\Delta\phi$) dependent eigen-energies are from the coupling of the states γ_{L1} , γ_{R2} , d_{\uparrow} and d_{\uparrow}^{\dagger} . To be more specific, the two Majoranas γ_{L1} and γ_{R2} couple commonly to the spin-up dot state, resulting in the ‘crossing’ structure at zero energy at $\Delta\phi = \pm\pi$, which is similar to the result of direct coupling of two Majoranas.⁴¹ It is just owing to this zero-energy crossing (at the Fermi energy) that the large Josephson current with abrupt jump is resulted in, in the presence of ‘relaxation’ or thermal equilibrium.

Second, for the dot level $\varepsilon_d \neq 0$ but $\theta = 0$ [see Fig. 5(d)], the Majorana states γ_{L2} and γ_{R1} have also the flat zero-energy (independent of $\Delta\phi$); however, the energies of d_{\downarrow} and d_{\downarrow}^{\dagger} move to ε_d and $-\varepsilon_d$, respectively. These would lead to an opening of the high-energy crossing at $\Delta\phi = 0$ (or $\pm 2\pi$), but still keeping the zero-energy crossings at $\Delta\phi = \pm\pi$ caused by γ_{L1} and γ_{R2} . As a result, the Josephson current keeps a large value and the jump survives, because the current are dominantly contributed by the zero-energy crossing states.

Third, if $\theta \neq 0$ and $\varepsilon_d = 0$ [see Fig. 5(a)], we see that the zero-energy degeneracy of γ_{L1} and γ_{R2} at $\Delta\phi = \pm\pi$ is removed. The disappearance of the zero-energy crossings leads to a strong reduction of the Josephson current and rounding the jump to smooth transition, as shown in Fig. 4(a).

Finally, for the case of both $\theta \neq 0$ and $\varepsilon_d \neq 0$, as shown in Fig. 5(b) and (c), the absence of efficient energy level interaction between the Majorana and QD states (owing to $\varepsilon_d \neq 0$) does not remove the zero-energy degeneracy of γ_{L1} and γ_{R2} at $\Delta\phi = \pm\pi$. Then, the zero-energy crossing structure of the energy spectrum at $\Delta\phi = \pm\pi$ results in a large Josephson current with abrupt jumps, despite that the dot level ε_d deviates far from the Fermi energy.

E. Effect of Majorana Interaction

Below we show that, in order to observe the featured behaviors discussed above, the overlap of the Majorana wavefunctions at the ends of the same nanowire should be negligibly small. Or, equivalently, the Majorana interaction should be negligibly small. In Fig. 6 we display the result for $\varepsilon_L = \varepsilon_R \neq 0$, which corresponds to nonzero coupling between the two Majoranas in the same nanowire. Indeed, we find that the amplitude of the Josephson current is strongly reduced and the jump disappears, with the increase of $\varepsilon_{L,R}$ [see Fig. 6(a) and (c)]. The basic reason is that the Majorana interaction in the same nanowire destroys the zero-energy Majorana state.

We have also checked that the large Josephson current with jump behavior cannot be restored by altering the dot level, even with ε_d in resonance with ε_L and ε_R [see Fig. 6(c) and (d)]. The reason is that, if $\varepsilon_L = \varepsilon_R \neq 0$, the zero-energy Majorana states γ_{L1} and γ_{R2} are destroyed and the zero-energy crossings at $\Delta\phi = \pm\pi$ disappear. As a consequence, the jumps at $\Delta\phi = \pm\pi$ are replaced by

rounded transitions, and the current is strongly reduced.

In Fig. 6(b) and (d), taking the current at $\Delta\phi = \pi/2$, we show again the θ dependence of current, in the presence of Majorana coupling ($\varepsilon_{L,R} \neq 0$). From this result we see clearly that, in order to obtain a larger supercurrent, we should make the nanowire longer than the superconductor coherence length to ensure the emergence of Majorana zero modes at the ends of the nanowire.

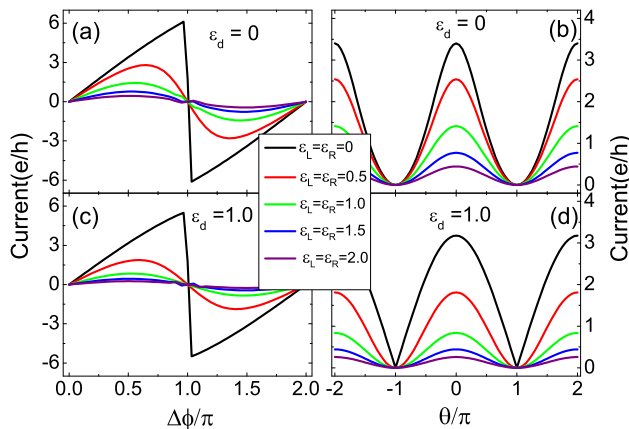


FIG. 6: (color online) (a) and (c): Effect of Majorana interaction (in the same nanowire manifested by nonzero $\varepsilon_{L,R}$), which would reduce the Josephson current and destroy the jump behavior at $\Delta\phi = \pm\pi$. (b) and (d): Nanowire-orientation-angle dependence of the current at $\Delta\phi = 0.5\pi$. Results for dot level $\varepsilon_d = 0$ and $\varepsilon_d = 1$ are presented, respectively.

F. 4π Periodic Current

So far we have assumed that the system always relaxes to a thermal equilibrium when we vary the phase difference $\Delta\phi$. In particular, at the zero-energy crossings at $\Delta\phi = \pm\pi$, this relaxation is accompanied by either an addition or a loss of a single particle, which therefore changes the parity of the particle numbers (i.e., the fermion parity). If such relaxation channel is blocked or the fermion parity is conserved, rather than the 2π periodic current we obtained above, a remarkable 4π periodic Josephson current can be expected, which is usually regarded as one of the most prominent Majorana signatures.

The 4π periodic current can be calculated as well by using Eq. (8), based on the following technique: When we increase $\Delta\phi$ after passing through $\pm\pi$, for the state occupation of the levels crossing at zero energy (the Fermi level) at $\Delta\phi = \pm\pi$, we replace the occupation of the lower level under the Fermi energy by its counterpart above the Fermi level (owing to the fermion parity conservation), while satisfying the condition of thermal equilibrium after this replacement.

The results of the 4π periodic current are shown in Fig. 7, for one period. Compared with the 2π periodic

current, we find that the jumps at $\Delta\phi = \pm\pi$ disappear for all the 4π periodic currents. However, for the case of $\theta = 0$ and $\varepsilon_d \neq 0$ similar jumps may appear *near* (but not *at*) $\Delta\phi = \pm\pi$, as observed in Fig. 7(b) and (c), owing to the accidental energy crossings at the specific phases. Again, along the increase of the angle θ , the amplitude of the current decreases. However, the current is more strongly suppressed in the case of $\varepsilon_d = 0$, while for larger deviation of ε_d (from the Fermi level) the current is less reduced.

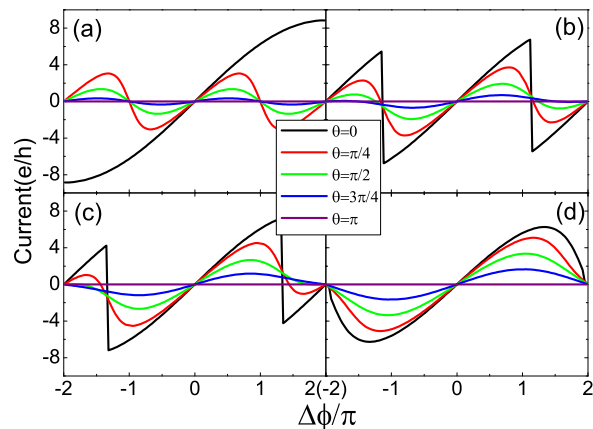


FIG. 7: (color online) The so-called 4π periodic current for a couple of set-up parameters, i.e., the nanowire-orientation-angles (as shown by the inset) and the dot levels (a) $\varepsilon_d = 0$, (b) $\varepsilon_d = 0.2$, (c) $\varepsilon_d = 0.5$, and (d) $\varepsilon_d = 1.0$.

IV. SUMMARY

To summarize, we have investigated the dc Josephson supercurrent through the Majorana-quantum dot-Majorana junction. Our particular interest is the consequence of the unique spin-selective coupling between the Majorana and dot states, which emerges only in the topological phase and will drastically influence the current through bent junctions and/or in the presence of magnetic fields in the dot area. Differing from the typical resonant tunneling behavior of the supercurrent through similar system in normal phase such as the superconductor-quantum dot-superconductor junction, we uncovered some counterintuitive results associated with the exotic nature of the Majorana fermion.

For instance, even for a straight junction and without magnetic field in the dot area, when the dot level deviates considerably from the Fermi energy, the Josephson supercurrent keeps a large amplitude of oscillation with the superconductor phase difference $\Delta\phi$ and reveals abrupt jumps of current at $\Delta\phi = \pm\pi$. Drastically, this result differs from the usual resonant tunneling behavior through similar system in normal phase. For a bent junction and/or in the presence of magnetic field in the dot, richer unexpected behaviors are found. In resonance

(the dot level aligned with the Fermi energy), we find that the supercurrent is to be strongly reduced by either the junction bending or the magnetic fields in the dot. At the same time, the current jumps at $\Delta\phi = \pm\pi$ are rounded. However, if the dot level deviates from the Fermi energy (i.e., violates the resonant tunneling condition), the supercurrent can, on the contrary, maintain a large amplitude of current and the current jumps robustly survive at $\Delta\phi = \pm\pi$, even under the influence of junction bending and magnetic fields in the dot. We expect these findings to be useful in future design of novel circuit devices based on quantum dots and Majorana nanowires.

Acknowledgements

This work was supported by NBRP of China (Grant No. 2015CB921102), NSF-China under Grants No. 11675016, No. 11274364 and No. 11574007, the Beijing Natural Science Foundation under No. 1164014, the China Postdoctoral Science Foundation funded project (Grant No. 2016M591103) and the Fundamental Research Funds for the Central Universities.

-
- * lixinqi@bnu.edu.cn
 † sunqf@pku.edu.cn
- ¹ E. Majorana, *Nuovo Cimento* **14**, 171 (1937).
 - ² F. Wilczek, *Nat. Phys.* **5**, 614 (2009);
 - ³ M. Franz, *Physics* **3**, 24 (2010).
 - ⁴ C. Nayak, S. H. Simon, A. Stern, M. Freedman, and S. Das Sarma, *Rev. Mod. Phys.* **80**, 1083 (2008).
 - ⁵ S. R. Elliott and M. Franz, *Rev. Mod. Phys.* **87**, 137 (2015).
 - ⁶ G. Moore and N. Read, *Nucl. Phys. B* **360**, 362 (1991).
 - ⁷ A. Y. Kitaev, *Phys. Usp.* **44**, 131 (2001).
 - ⁸ D. A. Ivanov, *Phys. Rev. Lett.* **86**, 268 (2001).
 - ⁹ M. T. Deng, C. Yu, G. Huang, M. Larsson, P. Caroff, and H. Q. Xu, *Nano Lett.* **12**, 6414 (2012).
 - ¹⁰ A. D. K. Finck, D. J. Van Harlingen, P. K. Mohseni, K. Jung, and X. Li, *Phys. Rev. Lett.* **110**, 126406 (2013).
 - ¹¹ E. J. H. Lee, X. Jiang, M. Houzet, R. Aguado, C. M. Lieber, and S. De Franceschi, *Nat. Nano.* **9**, 79 (2014).
 - ¹² V. Mourik, K. Zuo, S. M. Frolov, S. R. Plissard, E. P. A. M. Bakkers, and L. P. Kouwenhoven, *Science* **336**, 1003 (2012).
 - ¹³ Y. Oreg, G. Refael, and F. von Oppen, *Phys. Rev. Lett.* **105**, 177002(2010).
 - ¹⁴ R. M. Lutchyn, J. D. Sau, and S. Das Sarma, *Phys. Rev. Lett.* **105**, 077001(2010).
 - ¹⁵ G. Y. Huang, M. Leijnse, K. Flensberg, and H. Q. Xu, *Phys. Rev. B* **90**, 214507(2014).
 - ¹⁶ L. Fu and C. L. Kane, *Phys. Rev. Lett.* **100**, 096407 (2008).
 - ¹⁷ A. R. Akhmerov, J. Nilsson, and C. W. J. Beenakker, *Phys. Rev. Lett.* **102**, 216404 (2009).
 - ¹⁸ C. K. Chiu, M. J. Gilbert, and T. L. Hughes, *Phys. Rev. B* **84**, 144507 (2011).
 - ¹⁹ J.-P. Xu, M.-X. Wang, Z. L. Liu, J.-F. Ge, X. Yang, C. Liu, Z. A. Xu, D. Guan, C. L. Gao, D. Qian, Y. Liu, Q.-H. Wang, F.-C. Zhang, Q.-K. Xue, and J.-F. Jia, *Phys. Rev. Lett.* **114**, 017001 (2015).
 - ²⁰ S.-Y. Xu, N. Alidoust, I. Belopolski, A. Richardella, C. Liu, M. Neupane, G. Bian, S.-H. Huang, R. Sankar, C. Fang, B. Dellabetta, W. Dai, Q. Li, M. J. Gilbert, F. Chou, N. Samarth, and M. Z. Hasan, *Nat. Phys.* **10**, 943 (2014).
 - ²¹ M. Wimmer, A. R. Akhmerov, J. P. Dahlhaus, and C. W. J. Beenakker, *New J. Phys.* **13**, 053016 (2011).
 - ²² K. T. Law, P. A. Lee, and T. K. Ng, *Phys. Rev. Lett.* **103**, 237001 (2009).
 - ²³ A. R. Akhmerov, J. P. Dahlhaus, F. Hassler, M. Wimmer, and C. W. J. Beenakker, *Phys. Rev. Lett.* **106**, 057001 (2011).
 - ²⁴ K. Sengupta, I. Zutic, H.-J. Kwon, V. M. Yakovenko, and S. Das Sarma, *Phys. Rev. B* **63**, 144531 (2001).
 - ²⁵ J. Liu, A. C. Potter, K. T. Law, and P. A. Lee, *Phys. Rev. Lett.* **109**, 267002 (2012).
 - ²⁶ L. Fu and C. L. Kane, *Phys. Rev. B* **79**, 161408(R) (2009).
 - ²⁷ J. Alicea, Y. Oreg, G. Refael, F. von Oppen, and M. P. A. Fisher, *Nat. Phys.* **7**, 412 (2011).
 - ²⁸ S.-F. Zhang, W. Zhu and Q.-F. Sun, *J. Phys.: Condens. Matter* **25**, 295301 (2013).
 - ²⁹ J. J. He, T. K. Ng, P. A. Lee, and K. T. Law, *Phys. Rev. Lett.* **112**, 037001 (2014).
 - ³⁰ A Haim, E Berg, F. von Oppen, and Y. Oreg, *Phys. Rev. Lett.* **114**, 166406 (2015).
 - ³¹ T. Kawakami and X. Hu, *Phys. Rev. Lett.* **115**, 177001 (2015).
 - ³² H.-H. Sun, K.-W. Zhang, L.-H. Hu, C. Li, G.-Y. Wang, H.-Y. Ma, Z.-A. Xu, C.-L. Gao, D.-D. Guan, Y.-Y. Li, C. Liu, D. Qian, Y. Zhou, L. Fu, S.-C. Li, F.-C. Zhang, and J.-F. Jia, *Phys. Rev. Lett.* **116**, 257003 (2016).
 - ³³ S. Tewari, C. Zhang, S. Das Sarma, C. Nayak, and D. H. Lee, *Phys. Rev. Lett.* **100**, 027001 (2008).
 - ³⁴ D. E. Liu and H. U. Baranger, *Phys. Rev. B* **84**, 201308 (2011).
 - ³⁵ Y. Cao, P. Wang, G. Xiong, M. Gong, and X.-Q. Li, *Phys. Rev. B* **86**, 115311 (2012).
 - ³⁶ M. Lee, J. S. Lim, and R. Lopez, *Phys. Rev. B* **87**, 241402 (2013).
 - ³⁷ Q.-F. Sun and X. C. Xie, *J. Phys.: Condens. Matter* **21**, 344204 (2009).
 - ³⁸ Q.-F. Sun, B.-G. Wang, J. Wang, and T.-H. Lin, *Phys. Rev. B* **61**, 4754 (2000).
 - ³⁹ U. Meirav, M. A. Kastner, and S. J. Wind, *Phys. Rev. Lett.* **65**, 771 (1990).
 - ⁴⁰ Y. Meir, N. S. Wingreen, and P. A. Lee, *Phys. Rev. Lett.* **66**, 3048 (1991).
 - ⁴¹ P. Wang, J. Liu, Q.-F. Sun, and X. C. Xie, *Phys. Rev. B* **91**, 224512 (2015).